Received 23 September 2022; accepted 3 October 2022. Date of publication 6 October 2022; date of current version 14 October 2022.
The review of this article was arranged by Editor Z. Zhang.

*Digital Object Identifier 10.1109/JEDS.2022.3212395*

# The Gold Nanoparticles Enhanced ZnO/GaN UV Detector

**WENQING SONG[1,2], XIAOBIAO DAI[1], YINGKUN HE[1], AND TAO LI[1] (Member, IEEE)**

1 Key Laboratory of Hunan Province for Efficient Power System and Intelligent Manufacturing, Shaoyang University, Shaoyang 422000, China
2 School of Intelligent Manufacturing and Mechanical Engineering, Hunan Institute of Technology, Hengyang 421002, Hunan, China

CORRESPONDING AUTHOR: T. LI (e-mail: litao_0210@163.com)

This work was supported in part by the Natural Science Foundation of Hunan Province under Grant 2022JJ50170, and in part by the Project of College Student Innovation and Entrepreneurship Training under Grant S202210547034.

**ABSTRACT** Ultraviolet detectors can be used in ultraviolet disinfection, missile guidance and short-wave communication fields. Here we have grown GaN (002) film by chemical vapor deposition (CVD), through depositing 100 nm ZnO film as buffer layers on sapphire substrates by magnetron sputtering. Using Ni as the electrode, the metal-semiconductor-metal (MSM) ultraviolet (UV) detector was prepared. The device dark current, photocurrent and UV on/off current ratio were $5.19\times10^{-9}$A, $2.52\times10^{-7}$A and 54, under 2V bias. Then, using Au nanoparticles as plasmons, the photocurrent and photoresponsivity of the device were increased by 5.32 times and 5.25 times, respectively, and the UV on/off current ratio reached 176. The photoresponsivity of the device reaches the maximum value 0.42A/W at 370nm, the response time and relaxation time reach 0.1s and 0.12s, respectively.

**INDEX TERMS** ZnO/GaN film, UV detector, Au nanoparticles.

## I. INTRODUCTION

Ultraviolet detector can be used in space exploration, ultraviolet sterilization, missile guidance and short-wave communication fields. GaN has the characteristics of high electron mobility, high chemical stability, direct band gap, wide band gap, etc., and can be used for the preparation of high-power, high-speed optoelectronic components [1], [2], [3], [4]. There are many GaN preparation methods, such as metal organic chemical vapor deposition (MOCVD), molecular beam epitaxy (MBE), hydride vapor phase epitaxy (HVPE), CVD, etc [5], [6], [7], [8]. Among them, the quality of GaN films prepared by MOCVD is better and MOCVD is currently the most widely used, but the preparation cost is high [9]. Many researchers are exploring how to use low-cost CVD method to prepare high-quality GaN films. Ahmed et al. [10] reported the growth of single-crystal GaN on polycrystalline diamond at 975-1030 °C, and obtained complete lateral coverage and coalescence of GaN film. Lee et al. [11] reported smearing ZnO micro-nano structures on graphene substrates, and then using CVD to grow GaN to prepare LED devices. Mena et al. [12] reported the preparation of porous GaN epitaxial layers using CVD through the direct reaction of ammonia with gallium. The hydrophilic and hydrophobic properties of porous GaN epitaxial layer materials are discussed and explained using the Cassie-Baxter model. Ramírez-González et al. [13] reported that GaN films were prepared by a CVD system using GaAs (1 1 1) and ammonia as the reaction source and hydrogen as the carrier gas. In their report, the photoluminescence emission peaks changed from 420 nm to 384 nm and 372 nm as the temperature changed from 800 °C to 900 °C and 1000 °C.

There are many kinds of GaN-based UV detectors, among which MSM device has a simple structure, a mature manufacturing process, high photocurrent/dark current ($I_{ph}/I_{dark}$) ratio and a fast response time. Walker et al. [14] reported a MSM photodetector fabricated by GaN grown on sapphire and utilizing Pt/Au as electrodes. The UV/green contrast ratio of this device is about $1 \times 10^5$, and the response time is less than 10 ns. Wang et al. [15] reported the fabrication of tower-like GaN nanostructured MSM UV photodetectors using CVD system. The device has a photoresponsivity of 122.07 mA/W at 3 V bias, a rise time of less than 82 ms, and a decay time of 164 ms. Li et al. [16] reported a Ni/GaN/Au asymmetric MSM UV detector with a response at 0 V bias, it improved photoresponsivity when a positive

bias is applied to the Ni/GaN interface. However, when the Ni/GaN interface was negatively biased, the internal gain disappeared. Jain et al. [17] reported GaN-based symmetric electrode (Pt-Pt) and asymmetric electrode (Pt-Ag) MSM GaN UV photodetectors. The photoresponsivity of the symmetric electrode (Pt-Pt) and asymmetric electrode (Pt-Ag) MSM devices are 126 mA/W and 280 mA/W under 10 V bias, respectively. Chang et al. [17] reported a GaN MSM UV photodetector with high spectral response, the device exhibited low dark current and high spectral response at both room temperature and 150 °C. The device photoresponsivity increased by 280% after being enhanced with 80 nm Al nanoparticles. Zhao et al. [18], Song et al. [19], Ouyang et al. [20], Ning et al. [21], and Chen et al. [22] team used ZnO, GaN with other materials to form heterojunction devices, practiced self powered ultraviolet photoelectric sensing, and the UV responsivity, $I_{ph}/I_{dark}$, response time reached 9.7 mA/W, 690, 100 $\mu$s, respectively.

Gold nanoplasmons have enhanced effects in optoelectronic device applications. Chu et al. [23], Young et al. [24], Hsu et al. [25], and Young et al. [26] team used Au nanoparticles improved ZnO UV photodetectors, obtained responsivity and $I_{ph}/I_{dark}$ reached 14.8 mA/W, 1320, respectively. Xing et al. [27] coupled InGaN/GaN multiple quantum well nanorods with localized surface plasmons of gold nanoparticles, and time-resolved photoluminescence measurements confirmed that the emission enhancement originated from the coupling. Zhai et al. [28] demonstrated a normal-incidence quantum cascade detector excited by surface plasmon resonance using Au 2D hole arrays, and the results showed that Au 2D hole arrays resulted in enhanced quantum efficiency at most measurement temperatures, with a quantum efficiency enhanced 69% at 140 K. Dixit et al. [29] reported a device using Au nanoparticles sandwiched between two ZnO layers, which is suitable for UV-A, UV-B and UV-C detection, the device exhibits a high UV-to-visible rejection ratio of $1.32 \times 10^3$ and a UV-to-NIR rejection ratio of $8.79 \times 10^3$, with a photoresponsivity of 10.64 A/W ($\lambda = 315$ nm). Ikeda et al. [30] fabricated a two-electrode quantum dot-sensitized photoelectrochemical cell with gold nanoparticles, and the remarkable effect of the Au core stems from the enhanced excitation of the CdS shell and subsequent charge separation induced by a strong local electric field.

## II. EXPERIMENT

Since the GaN lattice constants a = 3.19 Å, c = 5.18 Å, and the sapphire substrate lattice constants a = 4.76 Å, c = 112.91 Å, if the GaN film is grown directly on the sapphire substrate by CVD, there will be 16% lattice mismatch rate. The lattice constants of ZnO are a = 3.25 Å, c = 5.21 Å, and the lattice mismatch rate with GaN is 1.9%. In order to explore the low-cost CVD growth of GaN films, a ZnO film was magnetron sputtered on the sapphire substrate as a buffer layer and then the GaN film was grown by CVD in this paper. Benefit from the matching of the ZnO buffer layer to the GaN lattice, the GaN film is mainly in the

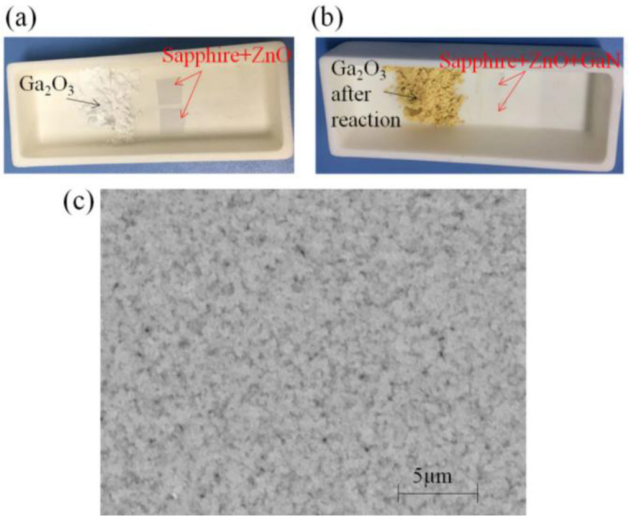


**FIGURE 1. (a) is the $Ga_2O_3$ powder and magnetron sputtering 100 nm thick ZnO substrate before CVD growth of GaN, (b) is the reaction source and ZnO/GaN film sample after CVD growth, (c) is the surface SEM image of ZnO/GaN film.**

002 lattice direction, and the MSM UV detector prepared by this film has a peak photoresponsivity at 370nm. Then, the performance of the device was enhanced by using gold balls as plasmons, and the photoresponsivity of the device was increased by Au plasmons.

Due to the low quality of GaN film grown directly on sapphire by CVD, a layer of about 100 nm thick ZnO film is sputtered on the sapphire substrate as the buffer layer by magnetron sputtering to grown GaN film. The sputtering power is alternating current 80W, the chamber air pressure is 1.4Pa, argon as carrier gas, and the sputtering time is 120mins. After the ZnO buffer layer was deposited on the sapphire substrate, the GaN film was grown by a CVD system. The conditions for CVD growth of GaN film is used $Ga_2O_3$ powder as the reaction source, the reaction temperature is 1000°C, ammonia gas is the reaction gas (100 sccm), the chamber pressure is maintained at about $1 \times 10^4$Pa, and the growth time is 40 minutes. Fig. 1(a) is the $Ga_2O_3$ powder and magnetron sputtering 100 nm thick ZnO substrate before CVD growth of GaN. Fig. 1(b) is the reaction source and ZnO/GaN film sample after CVD growth. The reaction source $Ga_2O_3$ reacted with ammonia at high temperature, the original white powder becomes pale yellow powder after the reaction. At the same time, a layer of GaN film was grown on the ZnO film, botained ZnO/GaN film. Fig. 1(c) is the surface SEM image of ZnO/GaN film, the SEM image shows that ZnO/GaN is a thin film material, and the film thickness is measured about 750 nm.

GaN film was grown on the 100nm ZnO film buffer layer by CVD. The surface roughness of the ZnO/GaN film was measured by an optical surface profiler (Wyko NT9100), the test area is 120 × 120 $\mu$m, and the optical image of ZnO/GaN film surface is shown in Fig. 2(a). The test values of the ZnO/GaN film surface roughness are shown in Fig. 2(b). The maximum deviation values ($\Delta$Z) in the X

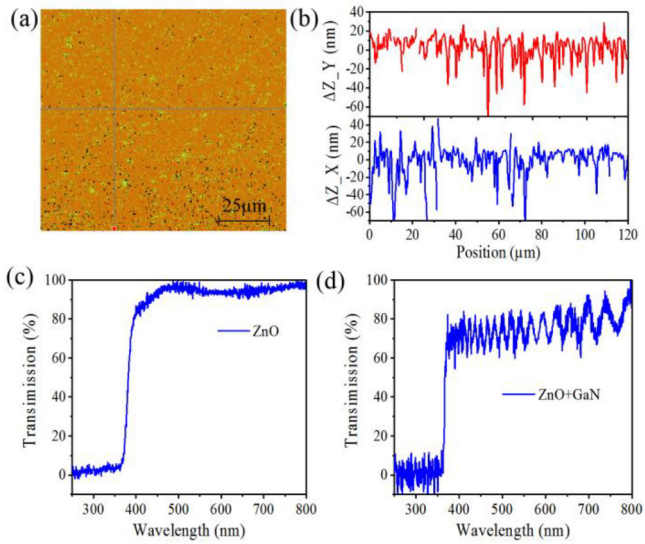


**FIGURE 2.** The ZnO/GaN film was tested by the optical surface profiler (a) and obtained the roughness values in X and Y direcions (b). (c) and (d) are the transmission tested results of ZnO and ZnO/GaN film.

and Y directions are both 60 nm, and the average variance Z in the X and Y directions is 3.7 nm and 1.2 nm, respectively. From the surface roughness measurement results, it can be seen that the surface roughness of the GaN film is about 1.2nm-3.7nm. From the test results, it can be found that the surface flatness of the GaN film is good, this is because the ZnO thin film buffer layer is deposited on the sapphire substrate, when the GaN film is grown by CVD, the ZnO buffer layer can better lattice match with GaN than sapphire, thus ensuring the surface flatness of the GaN thin film. Fig. 2(c) shows the transmission of the 100 nm ZnO film by magnetron sputtering on the sapphire substrate. The transmission drops rapidly at 360-390 nm, and the test result shows that the absorption peak of the ZnO film corresponds to 375nm. This is because the forbidden band width of ZnO is 3.3eV-3.4eV, so its absorption peak is at 365-375 nm. For above 410 nm waves, the transmission reaches more than 90%. This is because the thickness of the ZnO film is about 100 nm, and all the waves larger than the absorption peak range have high transmission. The transmission of ZnO/GaN is shown in Fig. 2(d), it drops rapidly around at 365nm, the forbidden band width of ZnO/GaN can be calculated as 3.4eV. This is because the thickness of the GaN film grown by CVD is much larger than that of the ZnO buffer layer, and the GaN film is on the surface of the ZnO film, so the transmission of the sample is mainly reflected of the GaN film. From Fig. 2(c) and (d), it can be found that the oscillation period of ZnO film transmission spectrum is longer, while the oscillation period of ZnO/GaN film is obviously smaller than ZnO film. This is because the oscillation period of transmission spectrum is inversely proportional to the film thickness. The thickness of ZnO film is about 100 nm, while the ZnO/GaN film reaches about 750 nm. Therefore, the oscillation period of ZnO/GaN film is smaller than ZnO film.

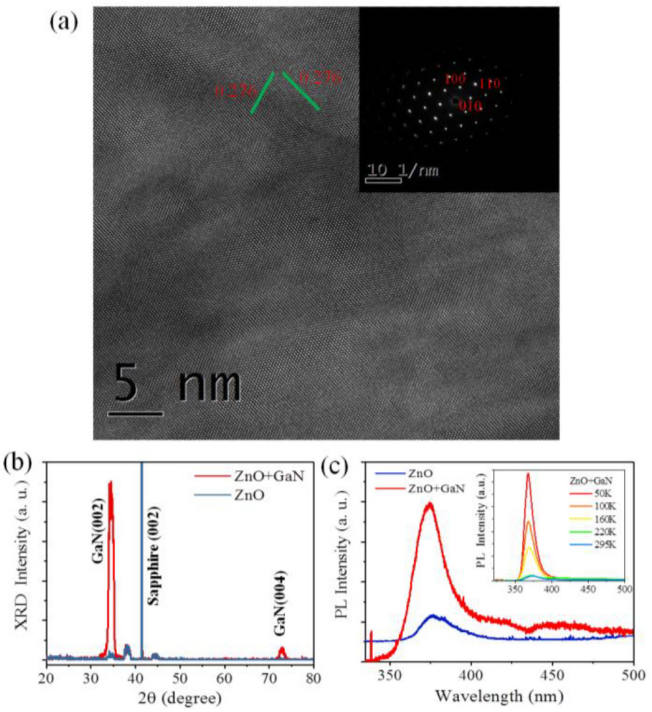


**FIGURE 3.** is the ZnO/GaN film material property test results. (a) is the HRTEM and SEAD tested results, (b) is the XRD tested results of ZnO film and ZnO/GaN film, (c) is the PL tested results of ZnO film and ZnO/GaN film at 295K, and the illustration is the ZnO/GaN tested at different temperature.

Fig. 3 shows the test results of ZnO/GaN film material properties. Fig. 3(a) is the high-resolution transmission electron microscopy (HRTEM) image and selected electron area diffraction (SEAD) image of GaN film which grown on ZnO film. From the HRTEM image of the GaN film, two crystal planes with a planar interval of 0.276nm are measured at an angle of 60 degrees. It is corresponding to the (100) and (010) crystal planes of wurtzite GaN [31], respectively, which further indicates that the material of the GaN film has a hexagonal wurtzite structure. Fig. 3(b) is the X-ray diffraction (XRD) tested results of ZnO film and ZnO/GaN film. Since the ZnO film is only 100 nm, its XRD test results show that there are smaller peaks around 34 degrees, 37 degrees and 45 degrees, corresponding to the 002, 101 and 102 crystal orientation of ZnO, respectively. The XRD test results of the ZnO/GaN film have a strong peak near 35 degrees, its full width at half maximum (FWHM) is 1.25 degree, indicating that the GaN film is mainly 002 lattice orientation. The XRD results of the ZnO film and the ZnO/GaN film have a very strong peak near 42 degrees, which is generated by the sapphire substrate. The photoluminescence (PL) spectrum of the ZnO film and ZnO/GaN film were shown in Fig. 3(c), the illustration is the ZnO/GaN film tested at different temperature. The photoluminescence spectrum test system is mainly composed of 325 nm He-Cd laser, HORIBA iHR550 spectrometer and a variable temperature control system, which can realize the variable temperature PL test from 10 K to 300 K. In

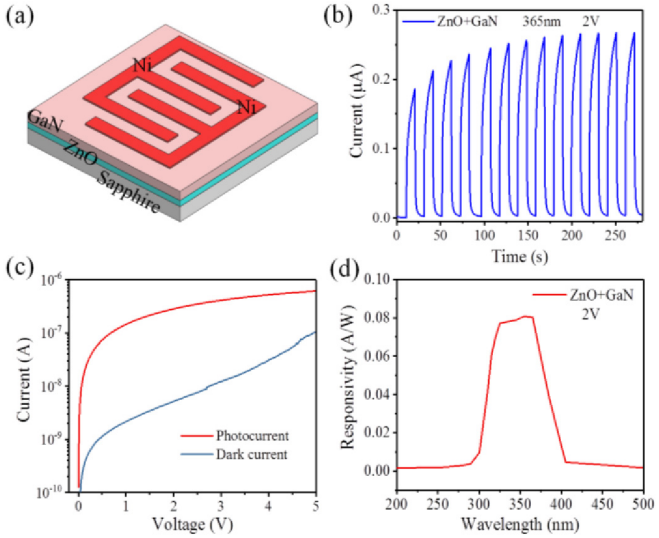


**FIGURE 4. (a) is the device structure diagram and (b) is the time-dependent photoresponse of ZnO/GaN film device. The dark current, photocurrent and responsivity of device are shown in (c) and (d).**

Fig. 3(c), the PL emission peak of ZnO film is about 375 nm, while the test peak of ZnO/GaN film is about 370 nm. The ZnO film peak is obviously weaker than ZnO/GaN film, this is because the ZnO film only 100nm, weaken the PL test result. During PL test with different temperatures, using a filter to remove yellow light, the PL luminescence peak around 370nm was observed, and the PL intensity gradually decreased with the increase of the test temperature, as shown in Fig. 3(c) illustration. As the ZnO film is only 100nm and the ZnO film PL emission peak is close to the GaN film PL emission peak, so in the test of ZnO/GaN film, the main performance is GaN film PL emission peak. The position of the PL emission peak is consistent with the near-band-edge emission of wurtzite GaN, which again proves the successful preparation of wurtzite GaN material. However, the corresponding wavelength of the PL test peak is 370 nm, and there is a red-shift phenomenon. This is because the growth thickness of the GaN film is only 750 nm, and there is a lattice mismatch with the ZnO film, which may lead to lattice defects in the GaN crystal, causing intra-lattice stress, resulting in a red shift of the PL test peak. The decrease of the PL intensity with the increase of temperature is related to the non-radiation recombination process. The increase of temperature will increase the proportion of the non-radiation recombination process, resulting in a decrease in the proportion of the radiation recombination process, that is, the PL luminous intensity decreases.

After the ZnO/GaN film is prepared, metal electrodes are deposited on the GaN film to form an MSM photodetector device. The MSM device fabrication consists of lithography, metal electrode Ni deposition and lift off. Ni was deposited by magnetron sputtering ($Ar_2$: 20 sccm, Pressure: 1.3 Pa, Power: dc power 60 W, Time: 30 minutes), with thickness to be around 0.3 $\mu$m. The MSM device structure is shown in Fig. 4(a), it contains sapphire substrate, 100 nm ZnO, 750 nm GaN and Ni electrode. The width and spacing of the interdigital electrodes are both 15 $\mu$m, and the overall area of the device is 400$\mu$m $\times$ 400 $\mu$m. Device's photoelectric performance were measured by Keithley 4200 SCS Parameter Analyzer at room temperature. The UV light source adopts a xenon lamp and a monochromator which can achieve 5 nm spectroscopy. The result of device time-dependent photoresponse as shown in Fig. 4(b). The time-dependent photoresponse of ZnO/GaN device was tested with 360 nm UV light turn on and off, under 2 V bias, the test time interval was 10 s. Within the 10-second time range, the photoresponse increased from the dark current value all the time, and did not reach the steady-state photocurrent value, the maximum photoresponse current in the fig. 4 (b) is 2.7 $\times$ $10^{-7}$ A. After the UV light was turned off, the current decreased rapidly and then slowly, and did not reach the steady-state dark current value during the test interval. It can be seen from Fig. 4 (b) that the maximum light response current of the device is gradually increasing in the previous 8 cycles, and the maximum current is stable at about 2.7 $\times$ $10^{-7}$ A until 8 cycles later. This is because there are some defects in the ZnO/GaN film, when external electrons enter the film material, some electrons are filled to the defect position. With the continuous introduction of external current, more and more defect positions in the film are filled, so the maximum current value displayed by the device is also increasing. Until the 8 cycle, the defect positions are completely filled, and the maximum test current displayed by the device is unchanged. Fig. 4(c) is the device dark current and photocurrent test results. Under 2 V bias, the device dark current and photocurrent are 5.19 $\times$ $10^{-9}$ A and 2.82 $\times$ $10^{-7}$ A, respectively, the device UV light source on/off current ratio is attained 54. As shown in Fig. 4(d), the photoresponsivity of the device reaches the peak value between 310-370 nm, which is about 0.08 A/W. The photoresponsivity peak corresponds to the wavelength of 370 nm, and there is also a red-shift phenomenon, which is consistent with the PL test results, further indicating that there are defects in the ZnO/GaN film.

In order to better improve the device performance, gold nanospheres are used as plasmons to enhance the device performance. The gold nanospheres are from XFNANO company, the diameter of the gold nanospheres is 40 nm. The aqueous solution of gold particles was spin-coated on the surface of the MSM device, and the spin-coating parameters were 600 r/min for 6 s and then 2000 r/min for 30 s. After spin coating, the SEM image of the device surface is shown in Fig. 5(a). With the gold plasmon enhances the device performance, the device time-dependent photoresponse test results under 2V bias are shown in Fig. 5(b). After the UV light source is turned on, the photoresponse current of the device rises rapidly and has a steady-state photoresponse current for the gold plasmon enhanced device. Similarly, after the UV light source is turned off, the device current drops rapidly to the dark current, and can reach the steady-state

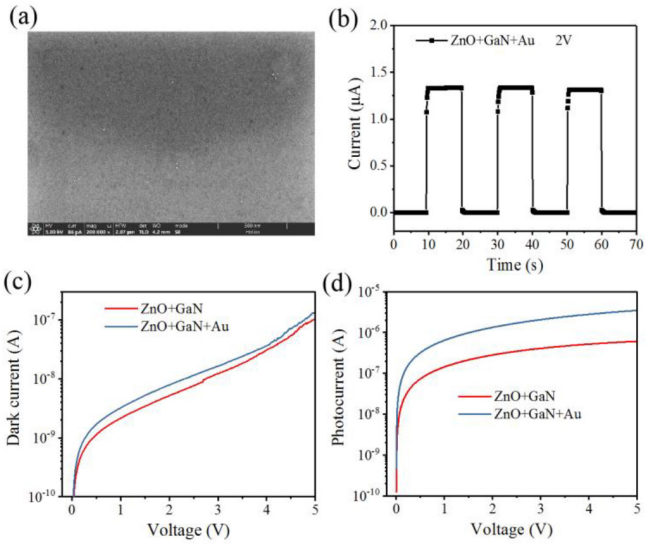


**FIGURE 5.** **is device performance test results after gold plasmon enhancement. (a) and (b) are the Au plasmons SEM image and the time-dependent photoresponse of ZnO/GaN device with Au plasmons enhancement. (c) and (d) are the comparison of dark current and photocurrent of ZnO/GaN film device and the device after Au plasmons enhancement under forward bias.**

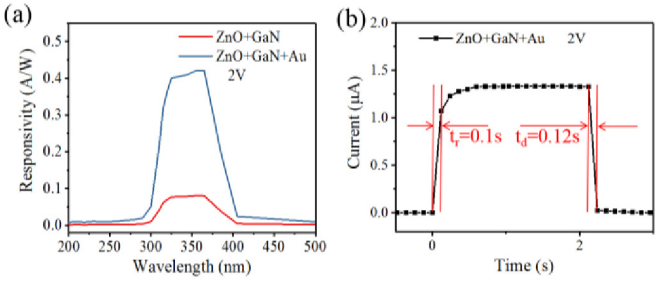


**FIGURE 6.** **(a) is the responsivity test results before and after gold plasmons enhancement, and (b) is the response time and relaxation time of Au plasmons enhancement device.**

**TABLE 1.** **The devices performance comparison.**

| Material | Responsivity (mA/W) | response time (s) | $I_{ph}/I_{dark}$ | Reference |
|---|---|---|---|---|
| $ZnO/Ga_2O_3$ | 9.7 | 0.0001 | 690 | [18] |
| ZnO+Au | 14.8 | - | 1320 | [23] |
| GaN | 280 | 0.014 | - | [32] |
| GaN | 219 | 0.047 | - | [33] |
| ZnO/GaN | 3200 | 0.159 | 2.87 | [34] |
| GaN+Au | 0.38 | 0.04 | ~$10^3$ | [35] |
| ZnO/GaN+Au | 420 | 0.1 | 176 | This work |

dark current value. As shown in the device time-dependent photoresponse test results, the device current increases from the steady-state dark current $7.56 \times 10^{-9}$ A to the steady-state photocurrent $1.33 \times 10^{-6}$ A. The device UV light source on/off current ratio is 176, and the steady-state photocurrent of the device with gold plasmon enhancement is 5.32 times of the maximum response current of the non-enhanced device. Fig. 5(c) and (d) are the comparison of dark current and photocurrent before and after gold plasmon enhancement of the device. Under 2V bias, the dark currents of the device without gold plasmon and the device with plasmon enhancement are $5.19 \times 10^{-9}$ A and $7.88 \times 10^{-9}$ A, respectively. The dark current of device with gold plasmon has increased, but it is still close to the dark current of device without gold plasmon. The photocurrents of the device without gold plasmon and the device with plasmon enhancement are $2.52 \times 10^{-7}$ A and $1.34 \times 10^{-6}$ A, under 2 V bias, respectively. Compared with the device without gold plasmon, the photocurrent is enhanced by 5.32 times.

## III. DISCUSSION

It can be seen from Fig. 5 that after adding gold nanoparticles, the photocurrent of the device increases significantly, but the dark current remains basically unchanged. In Fig. 5(b), during the time light response test, the photocurrent rises and reaches a steady state. In order to find the reason for the change of device performance before and after adding gold nanoparticles, the photoresponsivity, response time and relaxation time of the device with gold plasmon were tested as shown in Fig. 6. Fig. 6(a) shows the photoresponsivity of the device before and after gold plasmons enhancement, under 2 V bias, and the peak range of the photoresponsivity is 310-370 nm. The photoresponsivity reaches the maximum value at 370 nm, which is 0.08 A/W and 0.42 A/W, respectively. After gold plasmons enhancement, the photoresponsivity of the device is increased by 5.25 times. This is because under the action of metal plasmons, the optical responsivity is greatly improved, and the photocurrent is significantly increased. However, in the dark field, the metal plasmons do not work, so the dark current of the device is basically unchanged. Through the analysis of the time-dependent photoresponse test results after gold plasmon enhancement, as shown in Fig. 6(b), the photoresponse time and relaxation time are 0.1 s and 0.12 s, respectively. This indicates that the photocurrent can quickly enter the steady state after the gold nanoparticles enhance the photoelectric response of the device. Because the photocurrent is greatly increased, the photocarriers inside the device are collected in a short time, and then the photocarriers retained in the device are gradually collected. However, the retention amount only accounts for a small part of the collection amount in the early stage. Therefore, the device shows the phenomenon of rapidly entering the photocurrent steady state.

In order to better analyze the ZnO/GaN device performance, the performance parameters of this device are compared with the relevant device parameters reported in recent years. The comparison results are shown in Table 1. It can be seen that ZnO/GaN thin film devices grown by magnetron sputtering and CVD in this paper still have higher responsivity and $I_{ph}/I_{dark}$.

## IV. CONCLUSION

A GaN film with 002 lattice orientation was grown on sapphire substrate by using CVD system and ZnO film as buffer

layer. And using Ni metal as electrode, MSM UV detector was fabricated on ZnO/GaN film, the device has a peak responsivity of 0.08 A/W at 370 nm. Due to possible defects in the GaN film, the responsivity peak appears red-shifted to the absorption wavelength. Under 2 V bias, the dark currents and the photocurrent of the device are $5.19 \times 10^{-9}$ A and $2.82 \times 10^{-7}$ A, respectively. And the device UV light source on/off current ratio is 54. However, transient analysis found that the device response time and relaxation time were close to the measurement interval of 10 s. In order to improve the device performance, gold spheres with a diameter of 40 nm were used as plasmons, and the dark current, photocurrent and photoresponsivity of the enhanced device were $7.56 \times 10^{-9}$ A, $1.34 \times 10^{-6}$ A and 0.42 A/W, respectively. Benefiting from the effect of plasmons, the photocurrent and responsivity of the device are increased by 5.32 times and 5.25 times, respectively. Meanwhile, the response time and relaxation time of the device after plasmon enhancement are 0.1 s and 0.12 s, respectively.

## ACKNOWLEDGMENT

The authors declare no conflicts of interest. The data that support the findings of this study are available from the corresponding author upon reasonable request.

## REFERENCES

[1] S. K. Jain et al., "GaN-UV photodetector integrated with asymmetric metal semiconductor metal structure for enhanced photoresponsivity," *J. Mater. Sci. Mater. Electron.*, vol. 29, pp. 8958–8963, Mar. 2018.

[2] D.-H. Kim, D. Su Shin, and J. Park, "Enhanced light extraction from GaN based light-emitting diodes using a hemispherical NiCoO lens," *Opt. Exp.*, vol. 22, pp. A1071–A1078, Jun. 2014.

[3] B. Goldenberg et al., "Ultraviolet and violet light-emitting GaN diodes grown by low-pressure metalorganic chemical vapor deposition," *Appl. Phys. Lett.*, vol. 62, no. 4, pp. 381–383, 1993.

[4] Y. Huang et al., "Photocurrent characteristics of two-dimensional-electron-gas-based AlGaN/GaN metal-semiconductor- metal photodetectors," *Appl. Phys. Lett.*, vol. 96, no. 24, 2010, Art. no. 243503.

[5] J. Wang et al., "Investigation on minority carrier lifetime, diffusion length and recombination mechanism of Mg-doped GaN grown by MOCVD," *J. Alloys Compounds*, vol. 870, Jul. 2021, Art. no. 159477.

[6] C. Yang et al., "GaN vertical-channel junction field-effect transistors with regrown p-GaN by MOCVD," *IEEE Trans. Electron Devices*, vol. 67, no. 10, pp. 3972–3977, Oct. 2020.

[7] S. M. Islam et al., "Deep-UV emission at 219 nm from ultrathin MBE GaN/AlN quantum heterostructures," *Appl. Phys. Lett.*, vol. 111, no. 9, pp. 1–5, 2017.

[8] J. Mena et al., "Optical and structural characterisation of epitaxial nanoporous GaN grown by CVD," *Nanotechnology*, vol. 28, no. 37, 2017, Art. no. 375701.

[9] C. Xie et al., "Ultrawide-bandgap semiconductors: Recent progress in solar-blind deep-ultraviolet photodetectors based on inorganic ultrawide bandgap semiconductors," *Adv. Functio. Mater.*, vol. 29, no. 9, 2019, Art. no. 1970057.

[10] R. Ahmed, A. Siddique, J. Anderson, C. Gautam, M. Holtz, and E. Piner, "Integration of GaN and diamond using epitaxial lateral overgrowth," *ACS Appl. Mater. Interfaces*, vol. 12, no. 35, pp. 39397–39404, 2020.

[11] K. Lee, D. Yoo, H. Oh, and G.-C. Yi, "Flexible and monolithically integrated multicolor light emitting diodes using morphology-controlled GaN microstructures grown on graphene films," *Sci. Rep.*, vol. 10, Nov. 2020, Art. no. 19677.

[12] J. Mena, J. J. Carvajal, V. Zubialevich, P. J. Parbrook, F. Díaz, and M. Aguiló, "Tailoring wettability properties of GaN epitaxial layers through surface porosity induced during CVD deposition," *Langmuir*, vol. 37, no. 50, pp. 14622–14627, 2021.

[13] F. S. Ramírez-González et al., "Fabrication of $GaN_{(1-x)}As_x$, zinc-blende, or wurtzite GaN depending on GaAs nitridation temperature in a CVD system," *Cryst. Res. Technol.*, vol. 53, Jul. 2018, Art. no. 1800042.

[14] D. Walker et al., "High-speed, low-noise metal–semiconductor–metal ultraviolet photodetectors based on GaN," *Appl. Phys. Lett.*, vol. 74, no. 5, pp. 762–764, 1999.

[15] T. Wang, F. Cao, X. Ji, and Q. Zhang, "Study on tower-like GaN nanostructure: Growth, optical and fast UV sensing properties," *Superlatt. Microstruct.*, vol. 134, Oct. 2019, Art. no. 106233.

[16] D. Li et al., "Effect of asymmetric Schottky barrier on GaN-based metal-semiconductor-metal ultraviolet detector," *Appl. Phys. Lett.*, vol. 99, p. 7433, Jul. 2011.

[17] S. Chang, M. Chang, and Y. Yang, "Enhanced photoresponsivity of GaN metal-semiconductor-metal (MSM) photodetectors on GaN substrate," *IEEE Photon. J.*, vol. 9, no. 2, pp. 1–7, Apr. 2017.

[18] B. Zhao et al., "An ultrahigh responsivity (9.7 mA $W^{-1}$) self-powered solar-blind photodetector based on individual ZnO-$Ga_2O_3$ heterostructures," *Adv. Funct. Mater.*, vol. 27, no. 17, 2017, Art. no. 1700264.

[19] W. Song, J. Chen, Z. Li, and X. Fang, "Self-powered MXene/GaN van der waals heterojunction ultraviolet photodiodes with superhigh efficiency and stable current outputs," *Adv. Mater.*, vol. 33, no. 27, 2021, Art. no. 2101059.

[20] W. Ouyang, J. Chen, Z. Shi, and X. Fang, "Self-powered UV photodetectors based on ZnO nanomaterials," *Appl. Phys. Rev.*, vol. 8, no. 3, 2021, Art. no. 31315.

[21] Y. Ning, Z. Zhang, F. Teng, and X. Fang, "Novel transparent and self-powered UV photodetector based on crossed ZnO nanofiber array homojunction," *Small*, vol. 14, no. 13, 2018, Art. no. 1703754.

[22] Y. Chen, L. Su, M. Jiang, and X. Fang, "Switch type PANI/ZnO core-shell microwire heterojunction for UV photodetection," *J. Mater. Sci. Technol.*, vol. 105, pp. 259–265, Apr. 2022.

[23] Y.-L. Chu, Y.-H. Liu, T.-T. Chu, and S.-J. Young, "Improved UV-sensing of Au-decorated ZnO nanostructure MSM photodetectors," *IEEE Sensors J.*, vol. 22, no. 6, pp. 5644–5650, Mar. 2022.

[24] S.-J. Young and L. T. Lai, "Investigation of a highly sensitive Au nanoparticle-modified ZnO nanorod humidity sensor," *IEEE Trans. Electron Devices*, vol. 68, no. 2, pp. 775–779, Feb. 2021.

[25] C.-L. Hsu, H.-Y. Wu, C.-C. Fang, and S.-P. Chang, "Solution-processed UV and visible photodetectors based on Y-doped ZnO nanowires with $TiO_2$ nanosheets and Au nanoparticles," *ACS Appl. Energy Mater.*, vol. 1, pp. 2087–2095, Apr. 2018.

[26] S.-J. Young, Y.-J. Chu, and Y.-L. Chen, "Enhancing pH sensors performance of ZnO nanorods with Au nanoparticles adsorption," *IEEE Sensors J.*, vol. 21, no. 12, pp. 13068–13073, Jun. 2021.

[27] J. Xing et al., "Enhancement of emission of InGaN/GaN multiple-quantum-well nanorods by coupling to Au-nanoparticle plasmons," *J. Appl. Phys.*, vol. 123, no. 19, pp. 1–5, 2018.

[28] S.-Q. Zhai, J.-Q. Liua, F.-Q. Liu, and Z.-G. Wang, "A normal incident quantum cascade detector enhanced by surface plasmons," *Appl. Phys. Lett.*, vol. 100, no. 18, p. 1039, 2012.

[29] T. Dixit, J. Agrawal, S. V. Solanke, K. L. Ganapathi, M. S. R. Rao, and V. Singh, "ZnO/Au/ZnO configuration for high performance multiband UV photo-detection," *IEEE Sens. Lett.*, vol. 3, no. 9, pp. 1–4, Sep. 2019.

[30] T. Ikeda, R. Akashi, M. Fujishima, and H. Tada, "Plasmonic effect in Au(core)-CdS(shell) quantum dot-sensitized photoelectrochemical cell for hydrogen generation from water," *Appl. Phys. Lett.*, vol. 111, no. 11, 2017, Art no. 113901.

[31] W. Mao, K. Bao, R. Sun, Z. Li, and L. Rong, "Synthesis of hexagonal GaN nanoplates via a convenient solid state reaction," *J. Alloys Compounds*, vol. 620, pp. 5–9, Jan. 2015.

[32] S. Jain et al., "GaN-UV photodetector integrated with asymmetric metal semiconductor metal structure for enhanced responsivity," *J. Mater. Sci. Mater. Electron.*, vol. 29, Mar. 2018, pp. 8958–8963.

[33] N. Aggarwal et al., "Impact on photon-assisted charge carrier transport by engineering electrodes of GaN based UV photodetectors," *J. Alloys Compounds*, vol. 785, pp. 883–890, May 2019.

[34] L. Goswami et al., "Graphene quantum dots sensitized ZnO-Nanorods/GaN-Nanotowers heterostructure based high performance UV Photodetector," *ACS Appl. Mater. Interfaces*, vol. 12, no. 41, pp. 47038–47047, 2020.
[35] L. Goswami et al., "Au-nanoplasmonics-mediated surface plasmon-enhanced GaN nanostructured UV photodetectors," *ACS Omega*, vol. 5, no. 24, pp. 14535–14542, 2020.

**WENQING SONG** has been engaged in semiconductor material preparation and photoelectric device research for many years. His current research interests focus on III-nitride optoelectronic material and device.

**XIAOBIAO DAI** received the Ph.D. degree in mechanical engineering from Central South University (CSU), China, in 2021. From 2009 to 2014, he has been a Mechanical Engineer with SANY (Group Company Ltd.,) Research Institute. Since 2014, he has been a Lecturer with Shaoyang University. He is interested in computer vision and optoelectronic device.

**YINGKUN HE** is currently pursuing the bachelor's degree with the School of Mechanical and Energy Engineering, Shaoyang University, Shaoyang, China. His current research interests focus on III-nitride optoelectronic device.

**TAO LI** (Member, IEEE) was born in Shaoyang, Hunan, China, in 1988. He received the Ph.D. degree in mechanical engineering from Central South University, Changsha, China, in 2021. He currently works with the Key Laboratory of Hunan Province for Efficient Power System and Intelligent Manufacturing, Shaoyang University. His research interest focus on III-nitride optoelectronic material and device.